Hybrid Couplers in Bilevel Microstrip

Mark D. Prouty, *Student Member, IEEE,* and S. E. Schwarz, *Fellow, IEEE*

***Abstract*— Hybrid couplers can be built using a bilevel microstrip structure in which two strips are positioned broadside, one above the other. This simple geometry provides large coupling factors without the need for rigorous manufacturing tolerances. Remarkably, if the dielectric constant of one of the layers can be freely chosen, *ideal* hybrid coupler performance is achievable. Even when the choice of dielectric constant is constrained, good results can be obtained. A technique for achieving optimal design has been developed, and design curves are shown. Experiments confirm design predictions.**

The reentrant coupler may be analyzed as an interconnection of two bilevel couplers of the kind described here. This provides a simpler analysis than methods used earlier, and in some cases yields more accurate results.

I. Introduction

THERE has been recent interest in multilayer microstrip geometries, where there are two or more layers of conductors and dielectrics over a ground plane [1], [2]. Some common structures of this type, such as high-speed digital lines, have been analyzed [3], [4]. It is also interesting to study the properties of components built using the new geometry [5]–[8]. One such component is the hybrid coupler, a version of which has been reported experimentally [9]. In this paper, we study bilevel couplers numerically, report their properties, and give design data for couplers using different materials.

The geometry considered here is shown in Fig. 1. A principal advantage of this structure is the strong coupling possible between the conductors, without the tight lithographic tolerances necessary in the more common interdigitated coupler [10]. In other important properties, such as bandwidth, isolation, matching, and phase accuracy, we will show that this geometry has performance comparable to that of the more commonly used structures. In fact, if the designer is able to choose the exact value of dielectric constant for one of the layers, ideal coupler performance (perfect matching, isolation, and quadrature phase outputs, at all frequencies) is obtained.

We shall also consider in this paper cascaded sections of bilevel couplers. We will show that the reentrant coupler [11]–[13] may be analyzed as an interconnection of two bilevel couplers. Viewing this device as a cascade of elements, rather than as a single element, eases the computation and provides a more realistic analysis in certain cases.

A coupler with the geometry considered here is one of a class of nonsymmetric couplers. Many papers have been written considering properties of such devices [14]–[16].

Manuscript received May 18, 1992; revised February 16, 1993. This work was supported by the U.S. Army Research Office.

The authors are with the Department of Electrical Engineering and Computer Science and the Electronics Research Laboratory, University of California, Berkeley, CA 94720.

IEEE Log Number 9212727.

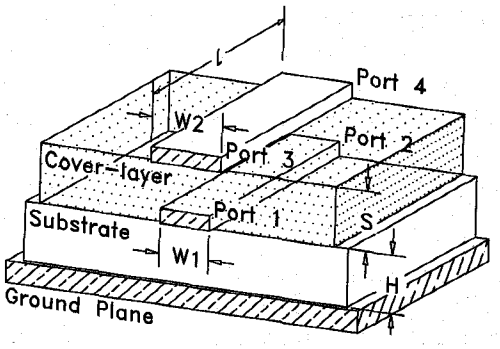

Fig. 1. The geometry of the bilevel coupler. Ports 1 and 4 are the isolated inputs, port 3 is the direct output for port 4, and port 2 is the direct output for port 1.

Usually, each line in a nonsymmetric coupler has a different impedance, and much of the literature centers around determining what impedance should be used to terminate each port [17], [18]. This difference in impedance might be considered an advantage, in order to effect an impedance transformation, but more often it will be disadvantageous, requiring another impedance matching element to convert back to the desired impedance [19]. The approach taken here, however, is to find the width of each line required to match all four ports to the same characteristic impedance.

II. Method of Analysis

The method used in this work follows the procedure outlined in [20]. It assumes quasi-TEM mode propagation, and lossless conductors and dielectrics. The telegraphist's equations describe the relationship between the current and voltage on the two coupled lines in terms of the mutual and self-capacitances and inductances of the lines. The eigenvectors of this system are the normal modes of propagation, corresponding to the even and odd modes for symmetric lines, while the eigenvalues are the propagation constants for each mode. The voltage and current along each line may be written as linear combinations of the normal modes. Some linear algebra then yields the 4-port impedance matrix Z of the coupler. Fairly simple closed-form expressions are given in [20] for the elements of Z. From them, the S-parameters may be readily determined.

The next step in the analysis is to find the capacitance and inductance matrices for the two conductors. These are found by twice solving for the 2-D electrostatic field. The capacitances are found from the charge on the conductors in the presence of dielectrics, while the inductances are found from the charges when the problem is solved with all dielectric constants equal to the free-space value. In order to solve for the static charges, we use the spectral domain method [21]. A

very similar geometry is considered in [22]. A straightforward generalization of that derivation yields the spectral Green's function necessary in our case.

III. Single-Stage Couplers

Using the above analysis procedure, we turn our attention to the design of hybrid couplers. Fig. 1 shows the port definitions used in this paper. Ports 1 and 4 are the isolated input ports, port 2 is port 1's direct output, and port 3 is port 4's direct output. Naturally, the structure is symmetrical with respect to swapping ports 1 with 2 and 3 with 4. In this paper, we are interested in designing couplers which are well-matched to 50 Ω lines at each port. This necessitates finding the optimal widths, W1 and W2, for the bottom and top conductors, respectively.

We use the following procedure to find the dimensions for desired coupling. First, the substrate and cover-layer dielectric constants are chosen as, presumably, these will be determined by the process the designer has available. Next, the separation S is set to some convenient value. This distance is treated as the independent variable in the design procedure. That is, once S is specified, the conductor widths required for best impedance match at all ports are found. The coupling coefficient is determined by these widths. Finally, the desired coupling coefficient may be obtained by adjusting S.

The conductor widths are found in the following manner. We wish to minimize the reflection coefficient at each port. Due to the symmetries in the problem, there are only two independent reflections: S_{11} and S_{44}. We need to find W1 and W2 which minimize both of these parameters. We are able to do this because S_{11} is only a weak function of W2, and S_{44} is only a weak function of W1. Therefore, the minimization problems are nearly independent, and may be solved by a simple iterative procedure. First, W2 is chosen arbitrarily, and then S_{11} is minimized as a function of W1. Then, W1 is held constant, while S_{44} is minimized as a function of W2. Fixing W2 now, and minimizing S_{11} again, is usually enough iterations. This is not a mathematically rigorous procedure, to be sure; it is not guaranteed to give S_{11} and S_{44} both near their global minima. In practice, however, it does yield small reflection coefficients at all ports.

The description has so far omitted one important point. The S-parameters are functions of the electrical length of the coupler, which is related to the speed of propagation of the normal modes. If both modes had the same velocity, the coupler would need to be a quarter-wavelength long [23]. However, when the velocities differ, due to the inhomogeneous medium, no simple relation exists to find the optimal length. We proceeded numerically, finding the length L for which the coupling between the lines is (locally) maximized. We then define an effective dielectric constant for the coupler according to

$$L = \frac{c}{4f_o\sqrt{\epsilon_{\text{eff}}}} \tag{1}$$

where f_o is the center-band frequency.

Results of our calculations for several cover-layer dielectric constants on a GaAs substrate are shown in Figs. 2–6.

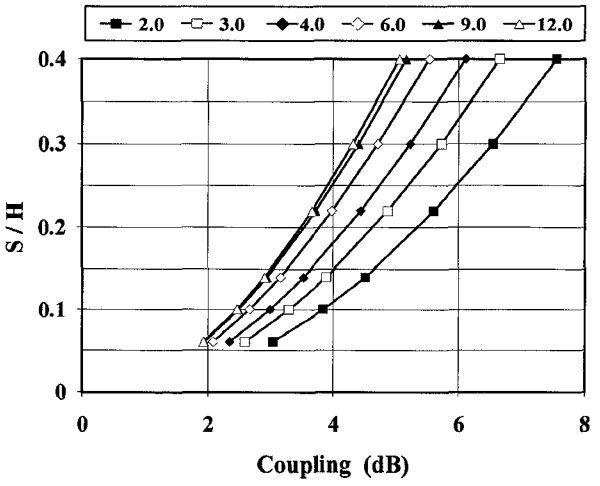

Fig. 2. Coupling magnitude at center frequency versus S/H for bilevel couplers built on GaAs. The legend refers to the dielectric constant of the cover-layer.

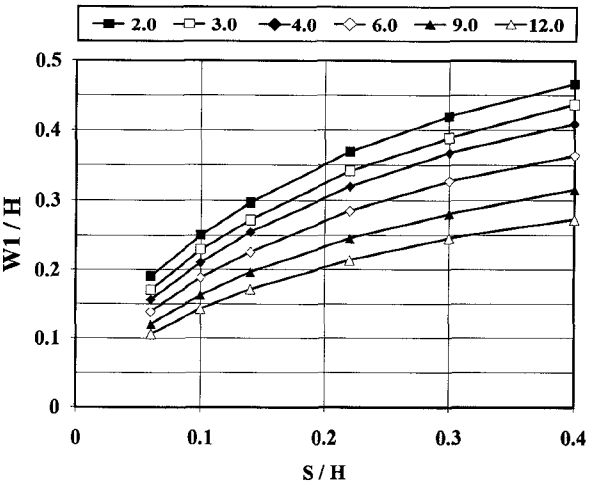

Fig. 3. Optimum lower conductor width versus separation (both normalized to H) for different cover-layer dielectrics.

The circuit designer may use these curves by first finding the separation needed to achieve the desired coupling for the material used. The graphs then show what matching is obtainable with those materials, and what conductor widths achieve this condition. The matching from the top port, S_{44}, and the isolation, S_{14}, are very similar in magnitude to S_{11}, so only S_{11} is plotted.

In most of these graphs, the quantity plotted varies monotonically with increasing ϵ_R of the cover-layer. The exception is Fig. 5, where matching performance is plotted. Rather than continuing to decrease, the return loss increases as the cover-layer ϵ_R is raised from 9.0 to 12.0. There appears to be a relationship between the dielectric constants of the layers for optimal matching performance. It turns out that at a certain value of cover-layer ϵ_R, a relationship exists between the capacitance and inductance parameters. That is (with the convention $C_m > 0$ adopted),

$$\frac{C_m}{\sqrt{C_1C_2}} = \frac{L_m}{\sqrt{L_1L_2}}. \tag{2}$$

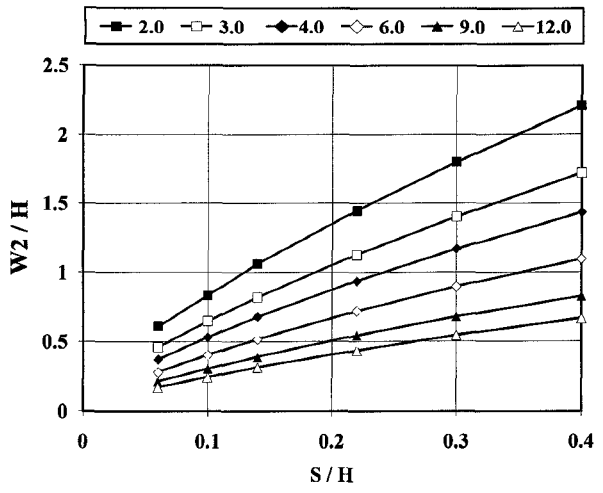

Fig. 4. Optimum upper conductor width versus separation (both normalized to H) for different cover-layer dielectrics.

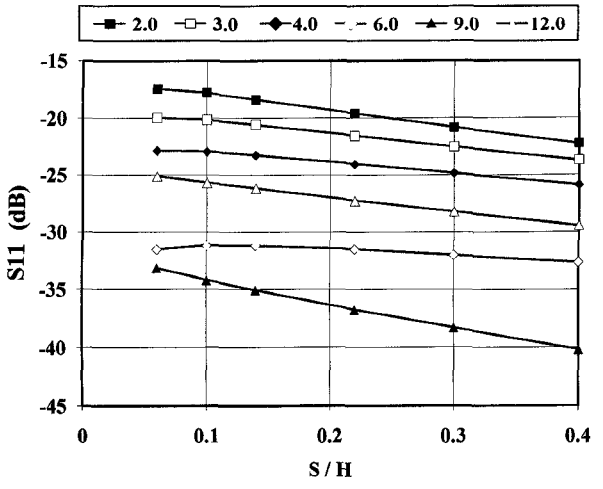

Fig. 5. Matching performance for couplers versus separation. S_{11} at the center frequency is plotted. S_{44} and S_{14} (isolation) are very nearly equal in magnitude to S_{11}

This relationship greatly simplifies the differential equations governing the wave propagation. Using the methods outlined in [24],[1] it can, in fact, be shown algebraically that the matching and isolation are perfect, and the output phases (after adding a length of transmission line to one of the outputs) are exactly 90° apart. Both characteristics hold at all frequencies.

The ideal cover-layer dielectric constant for different separations is shown in Fig. 6. Interestingly, where the cover-layer ϵ_R has its optimal value, we find that $\epsilon_{\text{eff}} = \epsilon_R$. This is quite remarkable, considering the enormously convoluted relationship between those parameters. No simple algebraic explanation of this equality has been found. Furthermore, (2) does not imply that the two mode velocities are equal. This differs from the case of symmetric couplers, where ideal coupling is obtained only when the even and odd mode velocities are equal [23]. In our case, such performance is obtained even when the normal modes have unequal velocity.

[1]Note that there is a sign error in [24, equations (14) and (15)]. Use equations (9) and (10) instead.

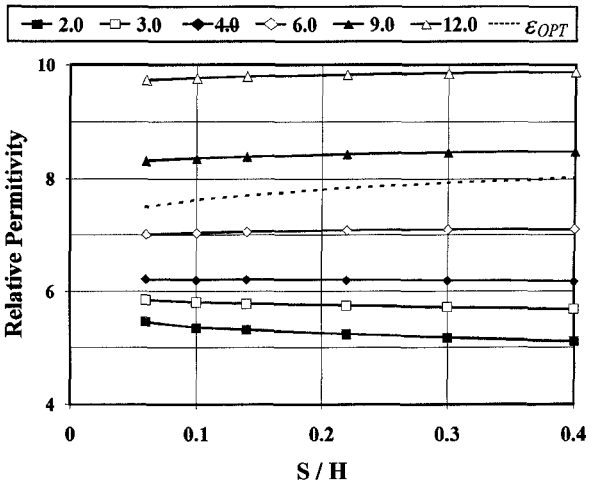

Fig. 6. The solid lines show the effective dielectric constant for the coupler for different cover-layer dielectrics. Using this value and equation (1), the coupler length may be determined. The dashed line shows the best cover-layer ϵ_R. At this value, ideal coupler performance is obtained.

Let us now consider the frequency-dependent properties of these couplers when built with commonly available materials. In this case, performance is not ideal, but is comparable to other single-stage coupler geometries. As an example, plots are shown in Fig. 7 for the polyimide ($\epsilon_R = 3.3$) on GaAs system. The magnitude of the direct and coupled outputs is similar to most 3-dB couplers, and the isolation and matching are reasonable. Of particular interest is the plot of the relative phases of the outputs. Note that from dc to beyond the center frequency, the phase diverges linearly from the desired quadrature response. This suggests that a length of transmission line could be added for correction, as shown in Fig. 8. The electrical length N of line may be calculated in the following way. If we define Sc_{ij} as the (i,j) component of the corrected S-matrix, and S_{ij} as the (i,j) component of the original S-matrix, one desires

$$90 = \angle\left(\frac{Sc_{13}}{Sc_{12}}\right) = \angle\left(\frac{S_{13}}{S_{12}}\right) - N \tag{3}$$

and

$$90 = \angle\left(\frac{Sc_{42}}{Sc_{43}}\right) = \angle\left(\frac{S_{42}}{S_{43}}\right) + N\,. \tag{4}$$

The first relation implies $N = \angle(\frac{S_{13}}{S_{12}}) - 90$, while the second requires $N = 90 - \angle(\frac{S_{42}}{S_{43}})$. These may both be satisfied if

$$\angle\left(\frac{S_{42}}{S_{43}}\right) + \angle\left(\frac{S_{13}}{S_{12}}\right) = 180\,. \tag{5}$$

In fact, this is a property of lossless, reciprocal 4-ports that are matched at all ports [19]. Thus, the same length of transmission line will correct the phases of the outputs for inputs to either the top or the bottom of the coupler. Fig. 7 also shows the difference in phases of the outputs after the transmission line has been added. The difference is within a few degrees of the desired quadrature relationship until, at higher frequencies, the network becomes poorly matched, and the above conditions no

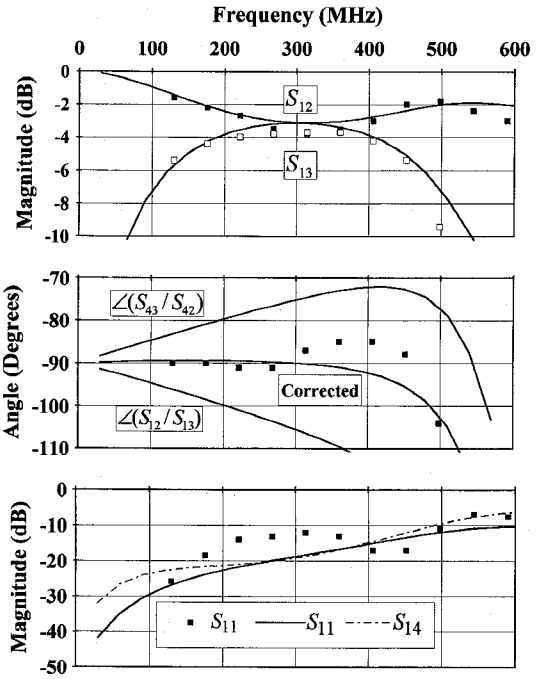

Fig. 7. Simulated and measured performance of a 3-dB coupler, with a cover-layer ϵ_R of 3.3 and substrate ϵ_R of 12.9, using W1/H = 0.27, W2/H = 0.59, S/H = 0.10, L = 10.55 cm, H = 0.635 cm. The points are the measured performance; lines are predicted. The "corrected" curve is the phase difference of the outputs after a correcting length of transmission line has been added, as shown in Fig. 8

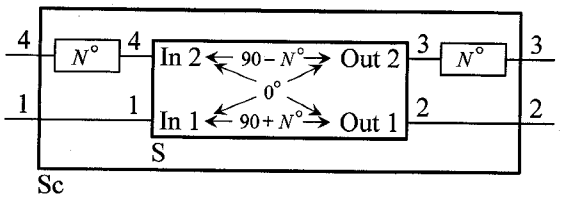

Fig. 8. Network diagram showing how to correct for phase error. The length of the transmission line N may be found in Fig. 9.

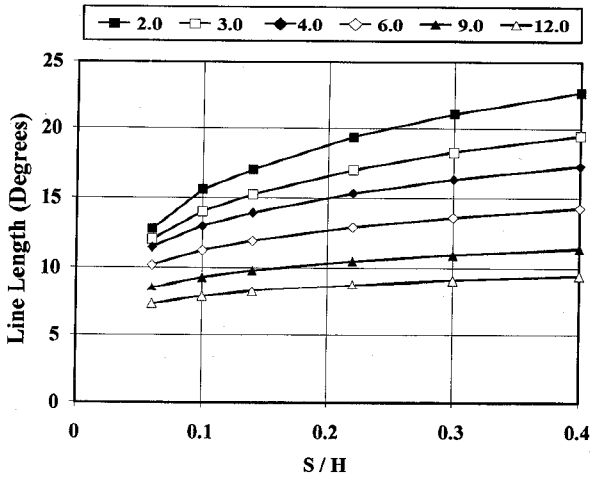

Fig. 9. Length of transmission line needed to correct for phase error as shown in Fig. 8.

longer hold. Fig. 9 shows design curves indicating the length of line necessary to correct the output phases.

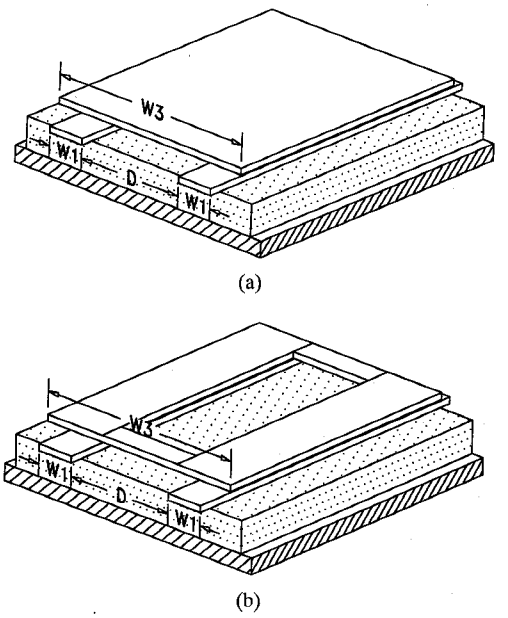

Fig. 10. Comparison of the geometries of the reentrant coupler (a) and the interconnected bilevel coupler (b). The top conductor is electrically isolated. The two lower conductors are the coupled lines.

Also shown in Fig. 7 are experimental data for a coupler built in the lab. Fairly low-frequency measurements were used to reduce the effects of the clumsy coax-microstrip connections. Reasonably good agreement is obtained.

IV. Reentrant Couplers

The reentrant coupler is a device for increasing the coupling between two conductors by using a third, floating conductor [25]. It has been adapted to stripline [11] and other planar configurations [12], [13]. The geometry of a planar reentrant coupler is shown in Fig. 10(a).

One way to analyze such a structure is to consider it as a single device, and analyze its entire cross section statically. In this method, which we shall call the reentrant method, the 3×3 capacitance and inductance matrices are calculated, then reduced to equivalent 2×2 matrices for the conductors of interest, using the assumption that the total current on the top conductor is zero [13]. However, analyzing a three-conductor problem is more complicated than analyzing a two-conductor problem, especially when using moment methods, since basis functions must be appropriately chosen for the third conductor.

Applying the analysis for the bilevel coupler to the reentrant case is accurate and has some advantages. Fig. 10(b) shows the physical geometry of two interconnected bilevel couplers, and Fig. 11 shows the connections schematically. It might seem that the division of the top conductor would give rise to a different current distribution and, thus, different performance. This is not the case in the quasi-TEM limit, however, since only longitudinal currents are assumed to exist. Since a simple network analysis is applied to find the overall response, we shall call this method the network method.

Results for simulations using the two different methods, shown in Figs. 12 and 13, reveal the differences in the analyses. In the network point of view, the two couplers do

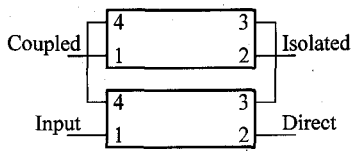

Fig. 11. Network diagram showing the connection of two single-stage couplers into the reentrant type of coupler. Ports 3 and 4 of each coupler form the isolated top conductor.

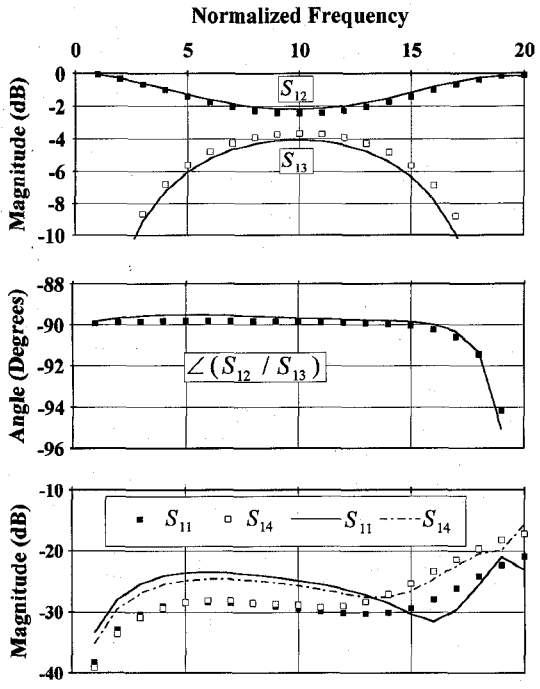

Fig. 12. Comparison of results using the reentrant type of calculation (points), and the cascaded network analysis (solid lines). $\epsilon_R = 2.1$ (both substrate and cover-layer), S/H = 13/200, W1/H = 120/200, W3/H = 332/200, $D = 68/200$.

not interact directly. Thus, this analysis will be closer to the reentrant analysis when the distance between the coupled lines is larger. This is seen by comparing the two figures.

There are some advantages to the network analysis, in addition to its computational simplicity. The network point of view allows for a delay to be simulated in the connection between the two couplers. This delay is assumed to be zero in the reentrant analysis. Thus, if the two coupled lines were widely spaced, the network analysis would lead to more accurate results. Furthermore, the network analysis predicts resonances in the top conductor, which are not predicted in the reentrant method of analysis. The reentrant method assumes the total current in the top conductor is zero at every transverse plane, and is thus oblivious to special behavior that arises when the coupler takes on a resonant length. For the case we have plotted, the resonant frequency is above the band of interest but, of course, this may not always be the case.

V. Conclusion

With development of multilevel circuits, couplers of the sort we have described, as well as other bi- and multilevel devices, can be expected to be of increasing practical interest.

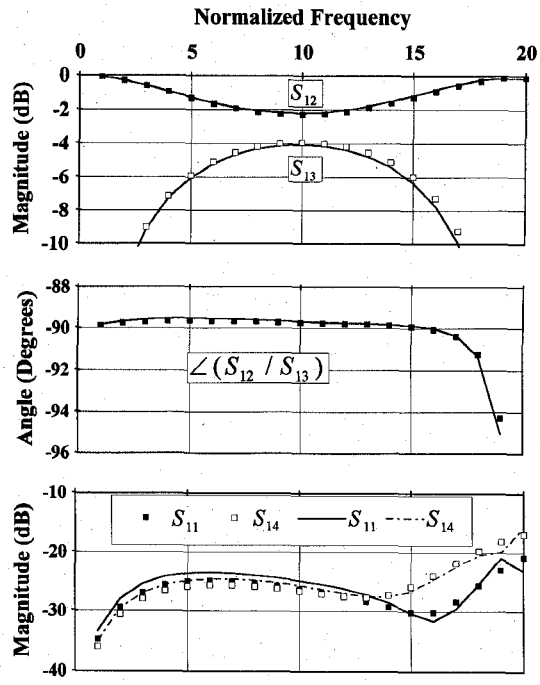

Fig. 13. Same as Fig. 12, except $D = 668/200$.

In this paper, we have supplied design data for bilevel couplers on GaAs. We have seen how having an additional dielectric constant available as a design parameter allows better optimization, even to the point of ideal performance. The couplers may be used either individually or in the convenient dual (reentrant) form.

References

[1] S. Banba, T. Hasegawa, and H. Ogawa, "Multilayer MMIC branch-line hybrid using think dielectric layers," *IEEE Microwave Guided Wave Lett.*, vol. 1, pp. 346–347, Nov. 1991.

[2] A. M. Pavio, A. Kikel, and S. K. Sutton, "Designing multiplayer ICs," *Appl. Microwave Mag.*, vol. 2, no. 4, pp. 75–81, Winter 1990.

[3] Y. Fukuoka, Q. Zhang, D. P. Neikirk, and T. Itoh, "Analysis of multilayer interconnection lines for a high-speed digital integrated circuit," *IEEE Trans. Microwave Theory Tech.*, vol. MTT-33, pp. 527–532, June 1985.

[4] J. P. K. Gilb and C. A. Balanis, "Asymmetric, multi-conductor low-coupling structures for high-speed, high-density digital interconnects," *IEEE Trans. Microwave Theory Tech.*, vol. MTT-39, pp. 2100–2106, Dec. 1991.

[5] Z. Chen and B. Gao, "Full-wave analysis of multiconductor coupled lines in MICs by the method of lines," *IEE Proc.*, vol. 136, pt. H, pp. 399–404, Oct. 1989.

[6] T. Chen, K. W. Chang, S. B. Bui, H. Wang, G. S. Dow, L. C. T. Liu, T. S. Lin, and W. S. Titus, "Broadband monolithic passive baluns and monolithic double-balanced mixer," *IEEE Trans. Microwave Theory Tech.*, vol. MTT-39, pp. 1980–1986, Dec. 1991.

[7] W. Schwab and W. Menzel, "On the design of planar microwave components using multilayer structures," *IEEE Trans. Microwave Theory Tech.*, vol. MTT-40, pp. 67–72, Jan. 1992.

[8] C. Tsai and K. C. Gupta, "A generalized model for coupled lines and its applications to two-layer planar circuits," *IEEE Trans. Microwave Theory Tech.*, vol. MTT-40, pp. 2190–2199, Dec. 1992.

[9] I. D. Robertson and A. H. Aghvami, "Novel coupler for gallium arsenide monolithic microwave integrated circuit applications," *Electron. Lett.*, vol. 24, no. 25, pp. 1577–1578, Dec. 1988.

[10] J. Lang, "Interdigitated stripline quadrature hybrid," *IEEE Trans. Microwave Theory Tech.*, vol. MTT-17, pp. 1150–1151, Dec. 1969.

[11] L. Lavendol and J. J. Taub, "Re-entrant directional coupler using strip transmission line," *IEEE Trans. Microwave Theory Tech.*, vol. MTT-13, pp. 700–701, 1965.

[12] J. A. G. Malherbe and I. E. Losch, "Directional couplers using semi-reentrant coupled lines," *Microwave J.*, pp. 121–128, Nov. 1987.
[13] M. Nakajima and E. Yamashita, "A quasi-TEM design method for 3-dB hybrid couplers using a semi-reentrant coupling section," *IEEE Trans. Microwave Theory Tech.*, vol. MTT-38, pp. 1731–1733, Nov. 1990.
[14] E. G. Cristal, "Coupled-transmission-line directional couplers with coupled liens of unequal characteristic impedances," *IEEE Trans. Microwave Theory Tech.*, vol. MTT-14, pp. 337–346, July 1966.
[15] R. A. Speciale, "Even- and odd-mode waves for nonsymmetrical coupled lines in nonhomogeneous media," *IEEE Trans. Microwave Theory Tech.*, vol. MTT-23, pp. 897–908, Nov. 1975.
[16] W. Marczewski, "The overlapped hybrid coupler design," in *Proc. 14th Euro. Microwave Conf.*, Liege, Belgium, Sept. 1984.
[17] V. K. Tripathi and Y. K. Chin, "Analysis of the general nonsymmetrical directional coupler with arbitrary terminations," *IEE Proc.*, vol. 129, pt. H., pp. 360–362, 1982.
[18] K. Sachse, "The scattering parameters and directional coupler analysis of characteristically terminated coupled transmission lines in an inhomogeneous medium," *IEEE Trans. Microwave Theory Tech.*, vol. MTT-38, pp. 417–425, Apr. 1990; and corrections, vol. MTT-39, p. 1252, July 1991.
[19] P. K. Ikalainen and G. L. Matthaei, "Wide-band, forward-coupling microstrip hybrids with high directivity," *IEEE Trans. Microwave Theory Tech.*, vol. MTT-35, pp. 719–725, Aug. 1987.
[20] V. K. Tripathi, "Asymmetric coupled transmission lines in an inhomogeneous medium," *IEEE Trans. Microwave Theory Tech.*, vol. MTT-23, pp. 734–739, Sept. 1975.
[21] D. Mirshekar-Syahka, *Spectral Domain Method for Microwave Integrated Circuits.* New York: Wiley, 1990.
[22] T. Itoh and A. S. Hebert, "A generalized spectral domain analysis for coupled suspended microstriplines with tuning septums," *IEEE Trans. Microwave Theory Tech.*, vol. MTT-26, pp. 820–826, Oct. 1978.
[23] R. Levy, "Directional couplers," in *Advances in Microwaves,* L. Young, ed., vol. 1, Academic Press, New York, 1966.
[24] M. K. Krage and G. I. Haddad, "Characteristics of coupled microstrip transmission lines—I: Coupled-mode formulation of inhomogeneous lines," *IEEE Trans. Microwave Theory Tech.*, vol. MTT-18, pp. 217–222, Apr. 1970.
[25] S. B. Cohn, "The re-entrant cross section and wide band 3-dB hybrid couplers," *IEEE Trans. Microwave Theory Tech.*, vol. MTT-11, pp. 255–258, July 1963.

Mark D. Prouty (M'87–S'89) received the B.A. degree in physics with honors form the University of Chicago in 1982, and the M.S. degree in electrical engineering from the University of California, Berkeley, in 1984.

He then joined Schlumberger Well Services in Houston, TX, to work on the development of advanced oil well induction measuring tools. In 1986 transferring to Fairchild Wellston's CCD Imaging Division, he worked on imaging sensors and video camera development. Since 1989 he has been pursuing the Ph.D. degree at the University of California, Berkeley. His broad research interests are currently directed toward numerical simulation of electromagnetic wave propagation, specifically in planar microwave circuitry.

Mr. Prouty received the Outstanding Graduate Student Instructor Award in 1991.

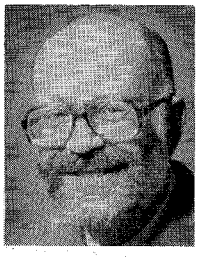

S. E. Schwarz (Sm'71–F'92) was born in Los Angeles, CA, in 1939. He received the B.S. degree in physics from California Institute of Technology in 1959, the A.M. in physics from Harvard University in 1962, and the Ph.D. degree in electrical engineering from CalTech in 1964.

He has held positions with Hughes Research Laboratories, AT&T Bell Laboratories, and IBM Research Laboratories. Since 1964 he has been a member of the Department of Electrical Engineering and Computer Sciences at the University of California, Berkeley, where he is a Professor. His research interests currently involve devices and techniques for planar microwave circuits.

Dr. Schwarz held a Guggenheim fellowship in 1971–1972. In 1990–1993 he occupied the President's Chair in Undergraduate Education at Berkeley.